INTERNATIONAL JOURNAL OF RESEARCH AND TECHNOPRENEURIAL INNOVATION
(IJRTI)

ISSN: XXXX - XXXX (Print); ISSN: XXXX - XXXX (Online)
Volume xx Issue xx (Month) 2024

Central Instrument Laboratory, University of Port Harcourt, Nigeria
E-mail: centralinstumentlaboratory@uniport.edu.ng

Green Synthesis of Iron-Nano-composite Capped by Ogbono Tree Leaves Extract to Remove 2-(N, N-dimethyl-4-aminophenyl) azobenzene carboxylic acid and Sodium-4-{[4-(dimethylamino) phenyl] diazenyl} benzene-1-sulfonate Colorants from Contaminated Water

Pereware Adowei[1,2]*, Sifon Emem Ebong[1], Gloria Ukalina Obuzor[1]

[1]Department Of Pure And Industrial Chemistry, Faculty Of Science, University Of Port Harcourt, Choba, P. M. B. 323, Port Harcourt, Nigeria

[2]Industrial Chemistry/Petrochemical Technology Option, School of Science Laboratory Technology, University of Port Harcourt, Choba, P. M. B. 323, Port Harcourt, Nigeria

Email address:

*Corresponding Author Email: *pereware.adowei@uniport.edu.ng*

ORCID ID: https://orcid.org/0009-0009-8973-5591

To cite this article:
Pereware Adowei, Sifon Emem Ebong and Gloria Ukalina Obuzor. Green Synthesis of Iron-Nano-composite Capped by Ogbono Tree Leaves Extract to Remove 2-(N, N-dimethyl-4-aminophenyl) azobenzene carboxylic acid and Sodium-4-{[4-(dimethylamino) phenyl] diazenyl} benzene-1-sulfonate Colorants from Contaminated Water. *International Journal of XXXXXX.* Vol. x, No. x, 2024, pp. x-x.

Keywords: Iron (III) oxide, Green synthesis; Adsorption; Methyl red; Methyl orange; Colorant, Ogbono tree

ABSTRACT

Lately, green synthetic procedure have been acknowledged as notable pathway in iron oxide synthesis due to their magnetic environment and ability be recovered from reaction concoction using external magnetic field. Moreso, several organic colorants in industrial effluents are toxic and require removal before discharge. Therefore, the objective of this paper was to synthesize green iron-nano-composite capped by ogbono tree leaves (Ig-nZVI) extract to remove 2-(N, N-dimethyl-4-aminophenyl) azobenzene carboxylic acid (MR) and Sodium-4-{[4-(dimethylamino) phenyl] diazenyl} benzene-1-sulfonate (MO) colorants from contaminated water using appropriate standard methods**.** The nano-composites were categorized by visual observation, Fourier transform infrared spectroscopy (FTIR) and scanning electron microscopy (SEM) respectively. Data obtained for adsorption study reveal that colourant removal was obtained at an optimal pH of 5. Colorant removal improved with increase in contact time, temperature and adsorbent doses to the maxima, then dropped thereafter. Freundlich isotherm model fitted the colorant removal process. Thermodynamic assessments show that removal of MR was endothermic, spontaneous while removal of MO was endothermic, spontaneous. These outcomes indicated that Ig-nZVI has prospects for removal of organic colorants in aqueous media. Hence, iron-nano-composite capped by ogbono tree (Ig-nZVI) leaves could also be advocated as a necessary, dependable, sustainable, and eco-friendly route to synthesize green nano-composites.

INTERNATIONAL JOURNAL OF RESEARCH AND TECHNOPRENEURIAL INNOVATION
(IJRTI)

ISSN: XXXX - XXXX (Print); ISSN: XXXX - XXXX (Online)
Volume xx Issue xx (Month) 2024
Central Instrument Laboratory, University of Port Harcourt, Nigeria
E-mail: centralinstumentlaboratory@uniport.edu.ng

1. INTRODUCTION

Green synthesis has evolved from the use of eco-friendly and sustainable production of nanoparticles without the use of non-environment friendly toxic chemical reagents in the laboratory. This process has gain tremendous attention in recent years using natural processes such as plants and microorganisms. One of the major encouraging and commonly flourishing subdivision of modern science and technology is the application of nanotechnology. The reason is because, nanoparticles show remarkable physicochemical and electromagnetic properties [1-10], These properties are essential in various scientific disciplines, such as catalysis, electronics, targeted drug delivery, water sensing and treatment, corrosion inhibition, oil recovery, and environmental and pollutant remediation in the industries and the Laboratory was the beginning of this great scientific innovation.

The synthesis of iron (III) oxide by using plants, bacteria, fungi and algae have been highlighted. iron (III) oxide produced by plants, fungi, bacteria and algae usually falls in 1–100 nm range and are of distinct shapes like cubic, tetragonal crystalline, spherical, cylindrical, elliptical, octahedral, orthorhombic, hexagonal rods, nanosphere and quasi spherical. Furthermore, these biomaterials play the roles of reducing, capping, stabilizing and fabricating agents in green synthesis of nanoparticles [11].

According to Kiwumulo [12] green synthesized iron (III) oxide nanoparticles from Ugandan grown Moringa Oleifera could be applied to targeted drug delivery systems because of their low cost, fast processing and nontoxicity. Also Abdulralman [13] used clove and green Coffee (g-Coffee) extracts to synthesize green iron oxide nanoparticles for the removal of Cd^{2+} and Ni^{2+} ions out of an aqueous solution. Buarki [14] synthesized iron oxide nanoparticles (α- Fe_2O_3) using *Hibiscus rosa sinensis* flower (common name, China rose) extract as a reducing and stabilizing agent. Selected researchers [15-21] had also used other abundant general low-cost materials which include natural materials, biologically derived materials, and agricultural industries waste materials.

However, the low-cost materials are problematic due to bulkiness in nature, slow adsorption kinetics, low capacity, disposal problems and re-generation, hence some authors have used activated carbon, hydrogen peroxide (H_2O_2), sodium hyperchlorite and other chemical agents for the textile industries effluents [22-25]. Consequently, adsorbents such as nanocomposites [26] and zerovalent metals [27-34] have become important for the removal of heavy metal ions, dyes and other pollutants from aqueous solution.

Extract from plants and plant materials as reducers and stabilizers has also been tried and found to be efficient in a single-step nanoparticle green synthesis process [35]. According to the authors Saif [35], this biogenic reduction of metal ion to base metal is pretty fast, readily conducted at room temperature and pressure, easily scaled up and are environmentally friendly. The reducing agents are water-soluble plant metabolites such as alkaloids, phenolic compounds, terpenoids and co-enzymes.

Many colorants used in several industries such as

textile, pharmaceuticals, food, cosmetics, plastics, paints, inks, photographs and paper industries produces large quantities of objectionable colored industrial effluents. These wastewater effluents contain dyes and other organic compounds that necessitate fast treatment owing to their toxic health and environmental effects [36-37]. Ogbono (*Irvingia gabonensis*) tree occurs freely in Nigeria and produces an edible fresh mango-like fruit [38-39]. The ogbono tree produces huge amount of leaf droppings as waste during the dry season. The fruit [40], seed [41], stem bark [42], and root [43] have been investigated for various uses other than food. However, research work on the use of the ogbono tree leaf as a reducing or capping agent for green synthesis is scanty.

Due to the paucity of data on the leaf, the objective of this paper was to synthesize green iron-nano-composite capped by ogbono tree leaves (Ig-nZVI) extract to remove 2-(N, N-dimethyl-4-aminophenyl) azobenzene carboxylic acid (MR) and Sodium-4-{[4-(dimethylamino) phenyl] diazenyl} benzene-1-sulfonate (MO) colorants from contaminated water.

2. MATERIALS AND METHODS

2.1. Courants

The colorants used are 2-(N, N-dimethyl-4-aminophenyl) azobenzene carboxylic acid (MR) and Sodium-4-{[4-(dimethylamino) phenyl] diazenyl} benzene-1-sulfonate (MO) as presented in figure 1a and b respectively. All chemical reagents used were of analytical grade.

2.2 Sample collection and Preparation

Ogbono tree (*Irvingia gabonensis*) leaves were collected and identified and washed several times with tap water and distilled water to remove dirt, bird droppings and other impurities and sun dried to remove residual moisture and finally grounded to powdery form and kept for further use as samples.

2.3 Aqueous Extraction of Ogbono Tree Leaves

Thirty (30.0 g) of finely rounded dried sample was placed in a 250 ml conical flask, 150 ml distilled water was added and placed in a water bath. The mixture was allowed to boil at 60 ^{0}C for 20 minutes. The aqueous plant extract was filtered with Whatman No. 1 filter paper and stored in a refrigerator at 4^{0}C for characterization and further use.

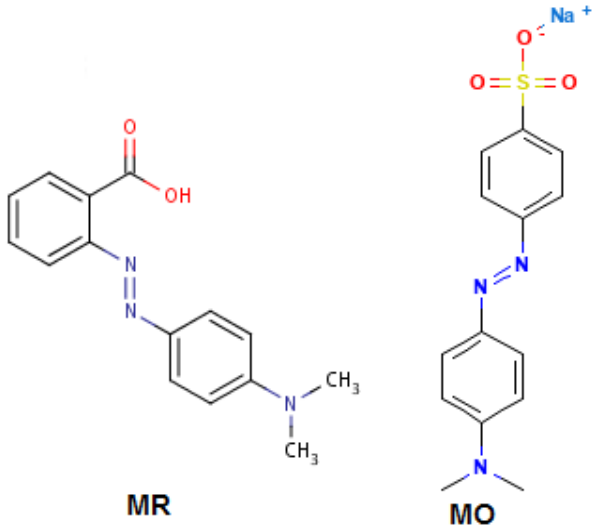

***Figure 1**: Structure of 2-(N, N-dimethyl-4-aminophenyl) azobenzene carboxylic acid [MR] and Sodium-4-{[4-(dimethylamino) phenyl] diazenyl} benzene-1-sulfonate [MO]*

2.4 Green synthesis of iron-nanocomposite capped by Ogbono tree (Irvingia gabonensis) Leaves (Ig) extract

10 ml Ogbono tree leaf extract (Ig) was added in dropwise to 90 ml 0.05 M $FeSO_4.7H_2O$ solution in a 250 ml conical flask on a magnetic stirrer. On addition of the first 4 drops of the plant extract the clear iron (II) solution immediately turned black. The reaction mixture was adjusted to pH 8 by adding in dropwise 1M NaOH solution. The reaction mixture was further stirred for 1 hour and later incubated at 60 ^{0}C in a water bath for 20 minutes to precipitate the Ig-nZVI. The reaction mixture was filtered through a whatman filter paper No.1 to obtain Ig-nZVI. The obtained Ig-nZVI was washed with distilled water and absolute ethanol.

The filtrate obtained was kept in the oven at 50 ^{0}C for 12 hours. After 12 hours, the synthesized Ig-nZVI (2.53 g) was collected and stored in a labeled sterile bottle for characterization and adsorption studies.

2.5 Preparation of Calibration Curves for the Dyes (MR and MO)

A stock solution of 1,000 mg L^{-1} was prepared by dissolving an appropriate 250 mg of MR and MO in separate 250 mL double-distilled water. Different concentrations of 5, 15, 25, 45, and 55 mg L^{-1} of dye were prepared from the stock solution. The sample concentrations were measured using a double beam UV-Vis spectrophotometer (U-2910, Hitachi, Tokyo, Japan) at laboratory temperature (27ºC ± 2ºC) at their maximum absorption wavelengths.

2.6 Batch Dye Elimination Studies

2.6.1 Effect of adsorbent dosage on Colorant elimination

To 10 ml of Colorant (MR and MO) with 20 mg/L concentration in two identical 100ml conical flask was added 0.02g 0.04g, 0.06g, 0.08g, 0.1g, 0.2g and 0.3g of Ig-nZVI and gently agitated for complete dispersion of the adsorbents with dye solutions and kept for 30mins. The reaction flask was again agitated after 30mins and filtered through Whatman filter paper number 1. The filtrates were stored in sterile plastic containers for determination of the final dye concentration using UV-Visible spectrometer.

2.6.2 Effect of initial concentration on Colorant elimination

The influence of initial *Colorant* concentration on adsorption was studied at room temperature. The concentration of each *Colorant* solution was varied from: 5, 10, 15, 20 and 25 mg/l respectively. A measured mass of 0.3g of Ig-nZVI was added to each initial concentration of dye solution. The mixture was agitated and equilibrated for 30 mins. The mixture was filtered and the filtrate collected into sterile plastic container for the determination of the final dye concentration using UV-Visible spectrometer.

2.6.3 Effect of pH on Colorant elimination

The *Colorant* solutions with 20 mg/L concentration (MR and MO) were pre-adjusted to pH 3, 5, 7, 9 and 11 with the addition of either 0.1M HCl or 1M NaOH solutions. To 10 ml of *Colorant* solution at the different pH, in two identical 100ml conical flask was added 0.3g of Ig-nZVI and gently agitated for complete mixture of the adsorbents with the *Colorant* solutions and kept for 30 min, thereafter, the mixture was agitated again and filtered with Whatman filter paper number 1 and the filtrates were stored in sterile plastic containers for UV-visible analysis.

2.6.4 Effect of time on Colorant elimination

To 10 ml of *Colorant* with 20 mg/L concentration solution in two identical 100ml conical flask, was added 0.3g of Ig-nZVI and gently agitated for complete mixture of the adsorbents with the *Colorant* solutions at room temperature (27^{0}C) and agitated again for 15 min, 30 min, 45 min, 60 min, and 75 min. At the end of each agitation time interval, the mixture was filtered using Whatman filter paper number 1 and the filtrate stored in sterile plastic containers for UV-visible spectroscopic analysis.

2.6.5 Effect of temperature on Colorant elimination

To 10 ml of *Colorant* with 20 mg/L concentration in two identical 100ml conical flask was added 0.3g of Ig-nZVI and gently agitated for complete mixture of the adsorbents with the *Colorant* solutions and transferred to a thermostat water bath which was pre-set at 30^{0}C, 45^{0}C, 60^{0}C, 75^{0}C and 90^{0}C for 30 min. The reaction flask was removed from the water bath and agitated and filtered through Whatman filter paper number 1. The filtrates were stored in sterile plastic containers for UV-visible analysis.

2.7 Mass Balance Calculations

The concentration of *Colorant* (mg/L) in the solution was measured by direct UV-visible spectrophotometric method using Genesis 20 Thermo Scientific at optimum wavelength. All the experiments were duplicated, and only the mean values were reported. The amount of *Colorant* eliminated at equilibrium by the Ig-nZVI, q_e (mg/g), were calculated by the mass balance relationship in equation 1:

$$q_e = \frac{C_O - C_e}{V} x\, W \qquad 1$$

Where C_O and C_e (mg/L) are the initial and equilibrium liquid-phase concentrations of *Colorant*, respectively, V is the volume of the solution (L), and W is the weight of nanocomposite used (g).

The percentage of *Colorant* eliminated from solution were calculated according to equation 2.

$$\%\,\text{Elimination} = \frac{C_O - C_e}{C_O} x100 \qquad 2$$

Where C_o (mg/L) is the initial *Colorant* concentration, C_e (mg/L) is the equilibrium concentration

2.8 Equilibrium Isotherm Models

Two equilibrium isotherm models were employed to evaluate the elimination of the colorants at different concentrations of MR and MO measured at room temperature under the experimental procedures for the effect of concentration.

The linearized Langmuir and Freundlich equilibrium isotherm model equations were used to describe the experimental data.

2.8.1 Langmuir Equilibrium Isotherm Model Equation

The linear form of the Langmuir equation used is presented in equation 3:

$$\frac{C_e}{q_e} = \frac{1}{K_L q_m} + \frac{1}{Q_m} C_e \qquad 3$$

Where q_m is the maximum monolayer capacity of the adsorbent (mg/g), K_L is the adsorption equilibrium constant (L/mg).

A plot of $\frac{C_e}{q_e}$ versus C_e is expected to give a slope of $\frac{1}{q_m}$ and intercept of $\frac{1}{K_L q_m}$; which will be used to evaluate the maximum monolayer capacity (q_m) and the adsorption equilibrium constant (K_L).

2.8.2 Freundlich Equilibrium Isotherm Model Equation

The linear Freundlich isotherm equation employed for the evaluation of the experimental data is given in equation 4.

$$\log q_e = \log K_F + \frac{1}{n} \log C_e \qquad 4$$

Where K_F is the Freundlich adsorption or distribution coefficient and represents quantity of dye adsorbed onto the adsorbent for unit equilibrium concentration and $\frac{1}{n}$ is the adsorption intensity of dye onto the adsorbent or surface heterogenecity, becoming more heterogeneous as its value gets closer to zero

The applicability of the Freundlich adsorption isotherm was also analyzed using the same set of experimental data, by plotting $\log q_e$ versus $\log C_e$.

2.9 Kinetics Models

Two kinetic models were used to study the kinetic behavior of the colorant measured at room temperature. The kinetics of *Colorant* (MR and MO) onto Ig-nZVI were analyzed using pseudo-first-order and pseudo-second order kinetic models.

2.9.1 Pseudo-first-order kinetic model equation:

The linearized form of the Lagergren pseudo-

first-order kinetic model equation used is presented in equation 5.

$$\log(q_e - q_t) = \log(q_q) - \frac{k_1}{2.303}t \qquad 5$$

Where q_e and q_t are the adsorption capacity at equilibrium and at time, t respectively (mg/g), $k_1$is the rate constant of pseudo-first order adsorption (L/min).

A plot of log (q_e – q_t) versus t will be used to evaluate the Langergren constants.

2.9.2 Pseudo-second-order kinetic model equation
The linear form of the pseudo-second-order equation (6) used is presented as

$$\frac{1}{q_t} = \frac{1}{k_2 q_e^2} + \frac{1}{q_e}t \qquad 6$$

Where k_2 (g/mg min) is the second order rate constant of the adsorption process

The linear plots were made using $\frac{1}{q_t}$ versus t

2.10 Thermodynamic Models

Thermodynamic parameters were computed from data obtained by measurement of temperature varied from 303 to 353 K. Thermodynamic parameters such as the thermodynamic equilibrium constant, K_e (Eqn. 7), change in standard Gibbs free energy, ΔG^o (Eqn. 8), change in standard enthalpy, ΔH^o (Eqn. 9), change in standard entropy, ΔS^o (Eqn. 10), and activation energy, E_a (Eqn. 11), were computed using the following equations:

$$K_e = \frac{q_e}{C_e} \qquad 7$$

$$\Delta G^O = -RT \ln K_e \qquad 8$$

$$G^O = H^O - T\Delta S^O \qquad 9$$

$$\ln K_e = \frac{\Delta S^O}{RT} - \frac{\Delta H^O}{RT} \qquad 10$$

$$\ln K_e = \ln A - \frac{E_a}{RT} \qquad 11$$

3. RESULTS AND DISCUSSION

3.1 Effect of Process Parameters on the Remove 2-(N, N-dimethyl-4-aminophenyl) azobenzene carboxylic acid and Sodium-4-{[4-(dimethylamino) phenyl] diazenyl} benzene-1-sulfonate Colorants from Contaminated Water

3.1.2 Effect of Adsorbent Dosage

According to Figure 2, the rate of removal of both colorants increased with increase in the adsorbent (Ig-nZVI) dose. At a dose of 0.02g, it was observed that 35.70% of MR colorant was removed by Ig-nZVI while that of MO was 27.33%. Subsequent doses of 0.04g, 0.06g, 0.08g and 0.1g correspondingly resulted in 48.10%, 71.40%, 88.61% and 94.17% removal of MR by Ig-nZVI. Results obtained for MO removal showed that at doses of 0.04g, 0.06g, 0.08g and 0.1g, the percentage removal increased to 57.17%, 78.10%, 82.2% and 89.00% for Ig-nZVI.

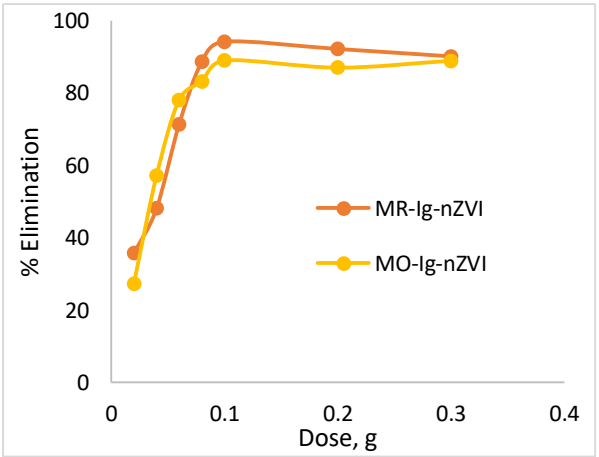

Figure 2: *Effect of Adsorbent Dose on removal of MR and MO with Ig-nZVI*

The increase in removal with increase in adsorbent dose occurred as a result of increase in the surface area available for colorant molecules to remove

[43]. The data showed that the percent removal becomes constant immediately after 0.1g adsorbent dose up to 0.3 g. Hence, the other experiments were conducted using an adsorbent dose of 0.3 g. This level was regarded as the saturation level.

3.1.2 Effect of Initial Colorant Concentration

The percentage removal of MR and MO by the adsorbent (Ig-nZVI) decreased with an increase in initial colorant concentration as shown in Figure 3. The removal rates of MR by Ig-nZVI was 98.5% when the initial concentration of MR was 5mg/L and its removal percentage reduced to 71.1% as the initial concentration was increased to10 mg/L. When the initial concentration was kept at 25 mg/L, the removal rate for Ig-nZVI dropped to 22.23%. In the case of MO, similar trend was observed; at initial concentration of 5 mg/L, 80.63% of MO was removed by Ig-nZVI. On increasing the initial concentration to 10 mg/L, percentage removal dropped to 51.60% for Ig-nZVI. In addition, when the initial concentration was kept at 25 mg/L, the removal rate for Ig-nZVI dropped to 27.00%. The decrease in the removal of both colorant in the aqueous media could be ascribed to surface saturation, consequently, leading to a decrease in percentage removal of both colorant corresponding to increasing initial concentration of both colorant. This observation agrees with the result reported by Siskova [37].

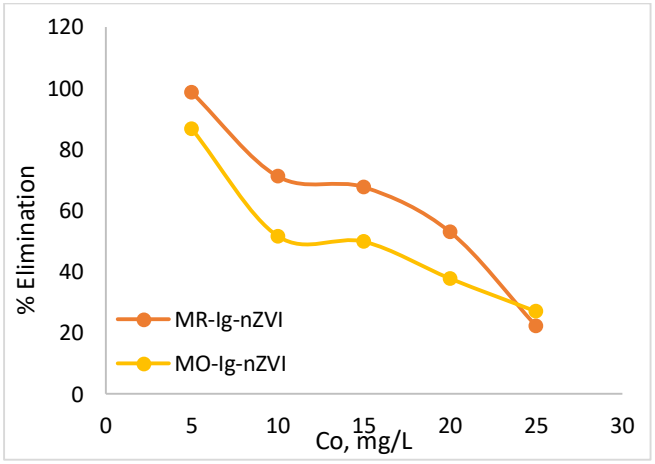

Figure 3: *Effect of Initial Concentration on removal of MR and MO with Ig-nZVI*

3.1.3 Effect of Time

At an initial contact time of 20 min (Figure 4), removal efficiency of Ig-nZVI for MR was fast with percentage removal of 48.97%. A similar trend was observed for MO, with percentage removal by Ig-nZVI at 33.5%. Percentage removal of MR at contact time 30-45min for Ig-nZVI increased from 61.40-72.93%. For MO, an increase in percentage removal was also observed at the same contact time range with values of 56.80-69.00% for Ig-nZVI. After 60 min, the removal percentage of MR by Ig-nZVI increased to 94.2% and that of MO increased to 79.77%. However, on increasing the contact time to 75min, there was no significant removal of both colorant. This result could be attributed to the fact that at the initial stage, there were large numbers of unoccupied sites on the surface of the adsorbents (Ig-nZVI) for adsorption. But as contact time increased, the unoccupied sites became saturated, which lead to slow pore diffusion of the MR and MO molecules onto the adsorbent (Ig-nZVI) and repulsion between the solid molecules and the bulk phases which is similar to the result of Karima [44].

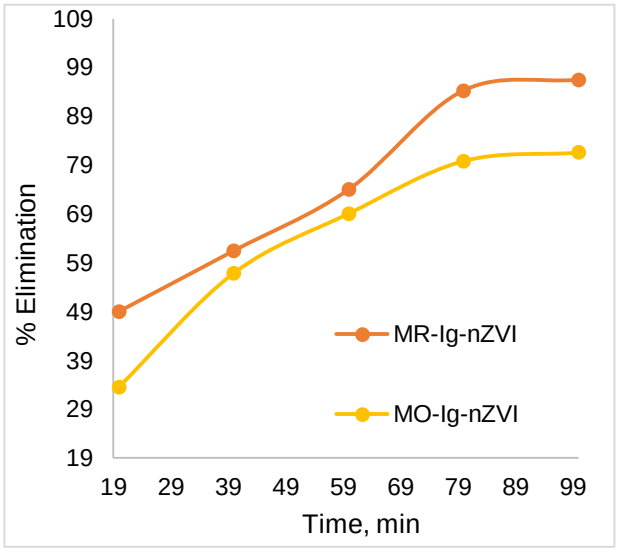

Figure 4: *Effect of Contact Time on removal of MR and MO with Ig-nZVI*

3.1.4 Effect of pH

During the removal process, functional groups, surface charges, degree of ionization and solubility

of adsorbent are important factors which are influenced by pH of the aqueous solution. Results obtained for the elimination of colorant at various pH (Figure 5) increased from pH 2 to a maximum at about pH 5.1 and gradually decreased to pH 11. Percentage removal of MR at pH 11, 9, 7, 5 and 3 were 37.3%, 41.5%, 50.3%, 80.33% and 54.6 respectively for Ig-nZVI. This is because at lower pH there were greater number of hydrogen ions present and thus, the degradation increased. The iron particles donate two electrons to the H^+ ions converting them into atoms which in turn attacks the colorant particles present in the wastewater, breaking them down to amines and rendering them colorless (Chatterjee *et al.*, 2010). Likewise, the percentage removal of MO from the aqueous medium increased with decreasing pH. At pH 5, the removal efficiency increased from 93.83% to 95.63% for Ig-nZVI.

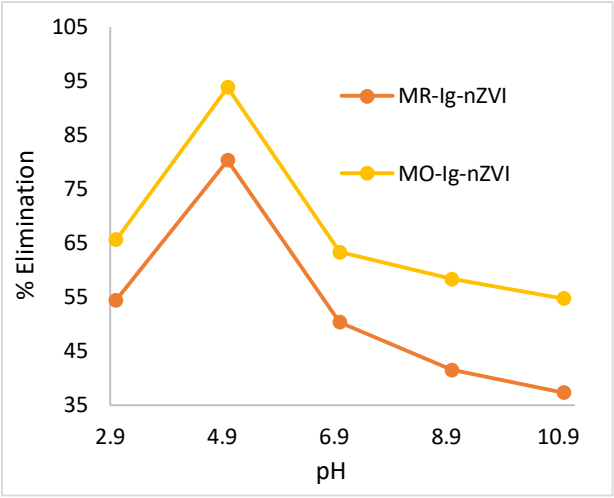

Figure 5: *Effect of pH on removal of MR and MO with Ig-nZVI*

Whereas increasing the pH of colorant solution to 7.0, 9.0 and 11 with the same amount of adsorbents (0.03g) at 27^{0}C and 10 min contact time a decrease in the removal of both colorant was observed with values of 63.33%, 58.30% and 56.90% respectively for Ig-nZVI. The low adsorption capacity at alkaline pH may be attributed to a decrease in reducing power of nanoparticles due to covering of nanoparticle with corrosion products; there is also a change in the charge of ZVI surface from positive to negative at alkaline pH which causes a repulsion force between the dye and nanoparticles [45].

3.1.5 Effect of Temperature

The removal of MR and MO by nanoparticle (Ig-nZVI) from aqueous media was controlled by temperature of the colorant solutions. The result as shown in Figure 6 was evident that colorants (MR and MO) removal increased with increase in the temperature of the reaction. This could be attributed to a reduction in the viscosity of the colorants solution so that the mass transfer resistance to the adsorbate in the boundary layer decreases [43]. The removal of MR by Ig-nZVI adsorbent was found to increase from 26.43% to 38.73 when the temperature was increased from 30^{0}C to 45^{0}C. On increasing the temperature further to 60^{0}C, 75^{0}C and 90^{0}C, Ig-nZVI gave removal percentages of 55.13%, 76.20% and 94.20%. Results obtained for the removal of MO by Ig-nZVI at temperatures 30^{0}C to 90^{0}C increased from 23.53% to 79.50%. The improvement in the removal of MR and MO could be attributed to a reduction in the viscosity of the dye solution so that the mass transfer resistance to the adsorbate in the boundary layer decreases. In addition, increase the rate of dispersion of adsorbate molecules in the inner pores of adsorbent particles [43, 46].

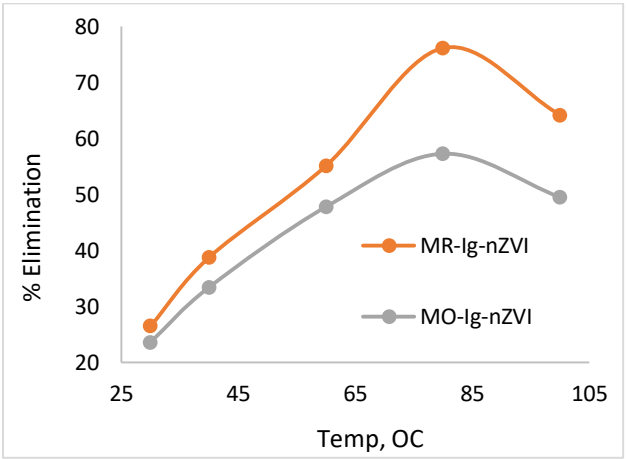

Figure 6: *Effect of Temperature on removal of MR with Ig-nZVI*

3.2 Equilibrium Isotherm Model

To relate the experimental data, two mono-component isotherm models; the Langmuir and Freundlich isotherm models were employed.

3.2.1 Langmuir isotherm

The Langmuir adsorption isotherm model explains the variation of adsorption of adsorbates with concentration. The linear expression of the Langmuir isotherm model as expressed in equation 3 was used to obtain figure 7.

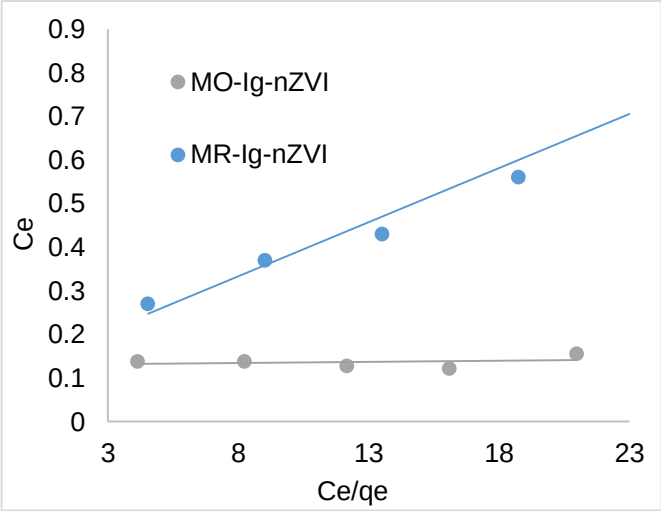

Figure 7: Langmiur isotherm of removal of MR and MO by Ig-nZVI

The Langmuir parameters obtained from Figure 7 are shown in Table 3. The removal of MR by Ogbono tree leaves-iron oxide-stabilized (Ig-nZVI) nanocomposite materials reveals that the Langmuir equilibrium constant, K_L (L/mg) related to energy of adsorption which quantitatively reflects the affinity between the adsorbent and adsorbate were computed as 0.079 (R^2 = 0.62) and 0.057 (R^2 = 0.845) for MR and MO respectively. These values implied that the removal process of MR and MO by Ogbono tree leaves extract-iron oxide-stabilized (Ig-nZVI) nanocomposite was both partially linear and perhaps may be unfavourable and the data did not fit well to the Langmuir isotherm model. Hence, it can be inferred that the capacity of Ogbono tree leaves extract iron oxide-stabilized (Ig-nZVI) nanocomposites to remove both MR and MO in aqueous system is low based on the Langmuir isotherm model.

Table 3. Langmuir Removal Equilibrium Isotherm parameters

	Langmuir Isotherm parameters		
Adsorbate-Adsorbents	q_{max} (mg/g	K_L L/mg)	R^2
MO-Ig-nZVI	40.02	0.184682	0.9598
MR-Ig-nZVI	166.7	0.046359	0.865

3.2.2 Freundlich isotherm

The Freundlich isotherm explains that the extent of adsorption. This empirical relationship describes the multilayer adsorption of heterogeneous systems and assumes that different sites have several adsorption energies involved [16]. The linear model of the Freundlich isotherm was used to logarithmically express as the experimental data (Figure 8). The Freundlich constants which gives an idea of the adsorption intensity and capacity, respectively were computed and are presented in Table 3

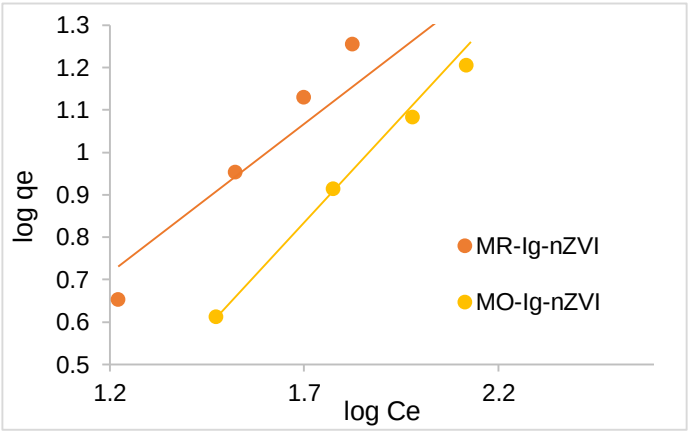

Figure 8: Freundlich isotherm of removal of MR and MO by Ig-nZVI

The results showed that, the degree of non-linearity between solution concentration and intensity of removal depends on the heterogeneity

which indicates the distribution of bonds and it is not dependent on the concentrations of adsorbents. The degree of non-linearity between solution concentration and adsorption depends on n as follows: If n = 1, the adsorption is linear; if n < 1, this implies that the adsorption process is chemical; if n > 1, the adsorption is a favorable physical process [47-49]. Data obtained from this study reveals that n values for MR and MO are greater than unity (Table 4). The higher values of n and R^2 for the adsorption of MR and MO onto Ig-nZVI implied that the adsorption process was a favorable physical process. These values also indicate the affinity of MR and MO molecules for the nano-adsorbents (Ig-nZVI). Hence it can be inferred that the adsorption of both MR and MO fitted well to the Freundlich isotherm model. A similar trend was observed by Shaibu [50].

Table 4. Freundlich Removal Equilibrium Isotherm parameters

	Freundlich isotherms parameters		
Adsorbate-Adsorbents	K_f $(mg/g)(L/mg)^{1/n}$	n	R^2
MO-Ig-nZVI	0.1682	1.009	0.9792
MR-Ig-nZVI	0.7473	1.425	0.8927

3.3 Comparison of Adsorption Capacities with Previously Reported Data

The adsorption capacities of Ogbono tree leaves extract-iron oxide-stabilized (Ig-nZVI) nanocomposite materials as well as of other adsorbents with respect to methyl red and methyl orange reported in the literature are presented in Table 5 and are compared with those obtained for this study. The ultimate adsorption capacities compared were those calculated from a Langmuir-type isotherm at 30 degrees and at an optimum solution pH of 8.0. It is palpable that the adsorption capacities vary within a wide range for the different adsorbents, depending on the experimental conditions. However, Ogbono tree leaves extract - iron oxide-stabilized (Ig-nZVI) nanocomposite materials were found to have strong potential regarding the removal of methyl red and methyl orange.

Table 5. Comparison of maximum elimination capacities with respect to MR and MO in the present study with those reported in the literature

Nano-composites	**q_{max}, mg/g**		**Reference**
	MR	**MO**	
CNT/Fe/CS composite	125	142.9	[51]
Cork Activated composite	-	16.66	[52]
PANI/glass composite	93	147	[53]
KOH-Activated polypyrrole-based	497.50	520.8	[54]
Chitosan/kaoli/γ-Fe_2O_3	36.67	35.27	[55]
Activated Pomelo peel waste	163.11	226.90	[56]
Potato peel powder	30.48	-	[57]
Phosphate Activated carbon	226.90	435.25	[58]
Amidoxine composite	-	142	[59]
Water hyacinth biomass	23.833	-	[20]
Ig-nZVI	166.7	128.21	This Study

3.4 Kinetics Models

To kinetic models were used in this study to investigate the controlling mechanism of removal processes. They are the pseudo-first-order (Figure. 9) and pseudo-second-order (Figure. 10) kinetic models respectively. The kinetic parameters for removal of MR and MO in aqueous solution by *Ogbono tree leaves extract*-iron oxide-stabilized (Ig-nZVI) nanocomposite materials are presented in Tables 6 and 7. The removal of the colorants by Ig-nZVI follows the pseudo-second-order kinetic model based on the higher R values, which relies on the assumption that chemisorption may be the rate-limiting step. In chemisorption, the colorant stick to the adsorbent surface by forming a chemical (usually covalent) bond and tend to find sites that maximize their coordination number with the surface [60]. The pseudo-second-order kinetic analysis reveals that the value of the initial removal rates (h) increases with increase in the initial colorant concentration. The lower the concentration

of colorants in the solution, the lower the probability of collisions between these species and, hence, the faster colorant molecules can bond to the active sites on the surface of the adsorbent [61].

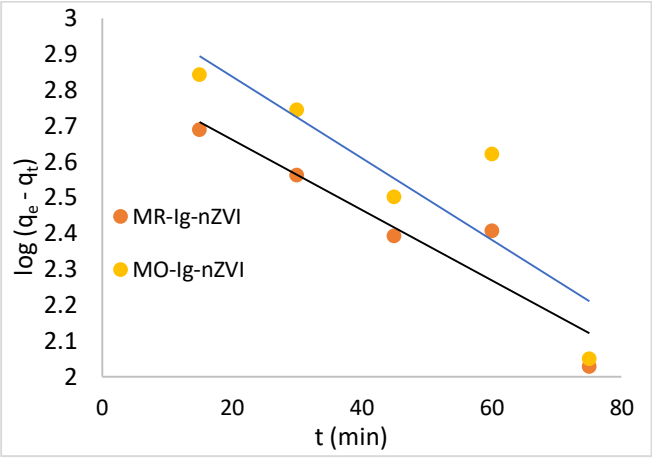

Figure 9: *Pseudo-first-order kinetic plot for MR and MO removal with Ig-nZVI*

Table 6. Pseudo first order Kinetic parameters for removal of MR and MO in aqueous solution by un-stabilized (nZVI) and *Ogbono tree leaves estract*-iron oxide-stabilized (Ig-nZVI) nanocomposite materials

	Pseudo first order	
Adsorbent	k_1(min^{-1})	R^2
MO-Ig-nZVI	0.026254	0.7663
MR-Ig-nZVI	0.022569	0.8841

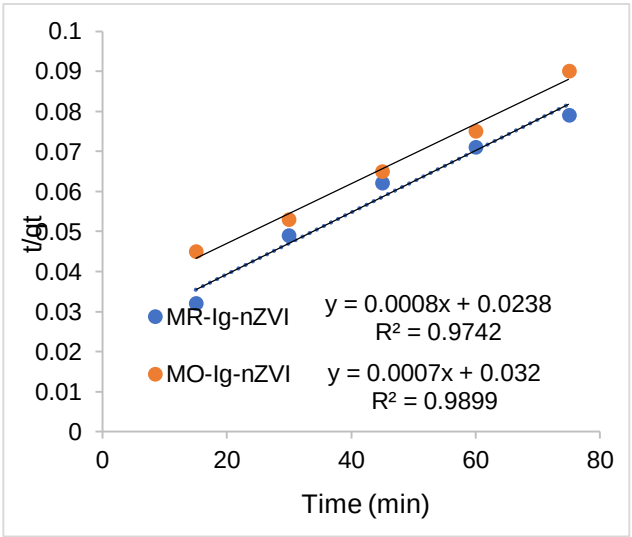

Figure 10: *Pseudo-second-order kinetic plot for MR and MO removal with Ig-nZVI*

Table 7. Pseudo second order Kinetic parameters for removal of MR and MO in aqueous solution by un-stabilized (nZVI) and *Ogbono tree leaves estract*-iron oxide-stabilized (Ig-nZVI) nanocomposite materials

	Pseudo second order	
Adsorbent	k_2 (g/mg^{-1} min^{-1})	R^2
MO-Ig-nZVI	89285.71	0.9899
MR-Ig-nZVI	105042	0.9742

3.5 Thermodynamics Studies

In order to evaluate the feasibility of the removal process, the thermodynamic and activation energy parameters such as free energy, enthalpy and entropy changes were evaluated from Figure 10 and the data presented in Table 8. The data obtained from the effect of temperature on the adsorption of MR and MO onto Ig-nZVI were tested with the adsorption thermodynamic equations. The thermodynamic parameters were the standard enthalpy change ΔH^0 (kJ mol^{-1}) and standard entropy change ΔS^0 (J mol^{-1} K^{-1}) were determined from the Van't Hoff plot calculated from the slope and intercept of the plots [62-63].

Table 8. The thermodynamic parameters

thermodynamic parameters	**Adsorbents**	
	MR-Ig-nZVI	MO-Ig-nZVI
ΔG^0 kJ/mol	-5.961	-5.341
ΔH^0 kJ/mol	88.74683	84.02434
ΔS^0 kJ/mol	-75.1813	-70.5055
Ea kJ/mol	-38.53532	-36.48473
R^2	0.9858	0.9485

A positive value of enthalpy change (ΔH^0) 88.75 kJmol^{-1} (Ig-nZVI) was obtained for the removal of MR onto Ig-nZVI. A positive ΔH^0 showed that the removal of MR onto Ig-nZVI was found to be endothermic. The standard entropy change (ΔS^0) values of -75.18 J K mol^{-1} (Ig-nZVI) obtained for MR removal onto Ig-nZVI indicated an increased degree of randomness at the solid–liquid interface during the adsorption of MR molecules onto Ig-nZVI while the negative values of the standard

Gibbs free energy (ΔG^0), 5.96 $KJmol^{-1}$ indicated the feasibility and spontaneity of the adsorption process of MR onto Ig-nZVI. Similarly, the positive ΔH^0 values of 84.02 $kJmol^{-1}$ for this study suggests that the adsorption of MO onto Ig-nZVI was endothermic. The standard entropy change (ΔS^0), -70.51 $JKmol^{-1}$(Ig-nZVI) indicated an increased degree of randomness at the solid–liquid interface during the adsorption of MO molecules by the adsorbates while the negative values of the standard Gibbs free energy (ΔG^0), 5.341$KJmol^{-1}$(Ig-nZVI) indicated the feasibility and spontaneity of the adsorption process of MO by Ig-nZVI. This result is similar to those reported by Hao [64] and Lisha [65].

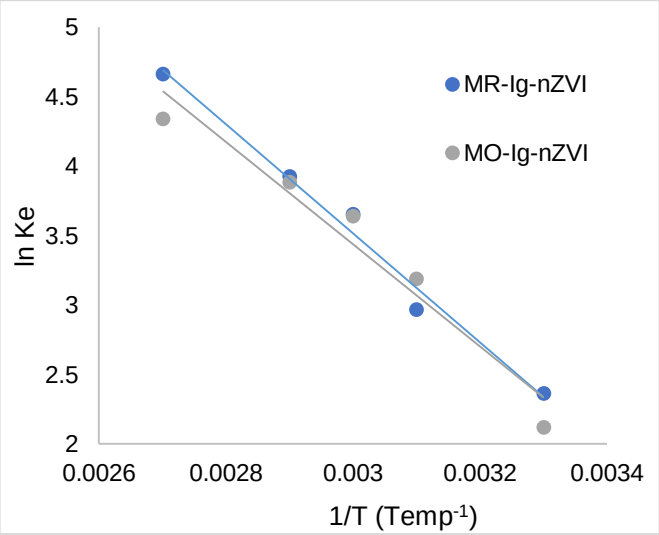

Figure 11: *Thermodynamic plot for MR and MO elimination with Ig-nZVI*

Colorant removal was found to be associated with strong electrostatic forces (physisorption), the overall process being slightly endergonic ($\Delta G^0 > 0$). Our study shows that Ig-nZVI has a great potential of removing dyes from wastewater and other dye-polluted aquatic systems.

4. CONCLUSION

Conclusively, green synthesis of Ogbono tree leave extract-iron nano-composite could be an effective one-step green alternative to the production of zerovalent iron nanoparticle for the removal of organic-based colorants in contaminated wastewater.

Conflict of Interest Declaration

The author(s) declare that there is no conflict of interest

References

[1] Chen, S., Yuan, R., Chai, Y., and Hu, F. (2013). Electrochemical Sensing of Hydrogen Peroxide Using Metal Nanoparticles: a Review. *Microchimica Acta* 180 (1), 15–32. doi:10.1007/s00604-012-0904-4

[2] Rastar, A., Yazdanshenas, M. E., Rashidi, A., and Bidoki, S. M. (2013). Theoretical Review of Optical Properties of Nanoparticles. J. Engineered Fibers Fabrics 8 (2), 155892501300800211. doi:10.1177/155892501300800211

[3] Pantidos, N., and Horsfall, L. E. (2014). Biological Synthesis of Metallic Nanoparticles by Bacteria, Fungi and Plants. J. Nanomedicine and Nanotechnology 5 (5), 1. doi:10.4172/2157-7439.1000233

[4] Arya, A., Mishra, V., and Chundawat, T. S. (2019). Green Synthesis of Silver Nanoparticles from green Algae (Botryococcus Braunii) and its Catalytic Behavior for the Synthesis of Benzimidazoles. *Chem. Data Collections* 20, 100190. doi:10.1016/j.cdc.2019.100190

[5] Hussain, M., Raja, N. I., Iqbal, M., and Aslam, S. (2019). Applications of Plant Flavonoids in the green Synthesis of Colloidal Silver Nanoparticles and Impacts on Human Health. Iranian J. Sci. Technol. Trans. A: Sci. 43 (3), 1381–1392. doi:10.1007/s40995-017-0431-6

[6] Saleh, T. A., Fadillah, G., and Saputra, O. A. (2019). Nanoparticles as Components of Electrochemical Sensing Platforms for the Detection of Petroleum Pollutants: A Review. Trac Trends Anal. Chem. 118, 194–206. doi:10.1016/j.trac.2019. 05.045

[7] Turan, N. B., Erkan,H. S., Engin, G. O., and Bilgili, M. S. (2019). Nanoparticles in the Aquatic Environment: Usage, Properties, Transformation and Toxicity—A Review. *Process Saf. Environ. Prot*. 130, 238–249. doi:10.1016/j.psep.2019.08.014

[8] Vasantharaj, S., Sathiyavimal, S., Senthilkumar, P., Lewis Oscar, F., and Pugazhendhi, A. (2019). Biosynthesis of Iron Oxide Nanoparticles Using Leaf Extract of Ruellia Tuberosa: Antimicrobial Properties and Their Applications in Photocatalytic Degradation. *J. Photochem. Photobiol. B: Biol.* 192, 74–82. doi:10.1016/j.jphotobiol.2018.12.025

[9] Adowei, P. (2024). Effect of Refluxing Time and Kinetics of Synthetic Organic Chemicals Removal in Aqueous Solutions by Carbons Produced from Nipa Palm Fronds. *American Journal of Applied and Industrial Chemistry*, *8*(1), 14-22. https://doi.org/10.11648/j.ajaic.20240801.12

[10] Adowei, P; Ebong, SE; Obuzor, GU (2021). Equilibrium, Kinetic and Thermodynamic Studies of Dyes in Aqueous Solution onto Iron Nanocomposite Stabilized by *Irvingia gabonensis* Leaf Extract. *J. Appl. Sci. Environ. Manage.* Volume. 25 (12) 2071-2083

[11] Priya, Naveen, Kaur K and Sidhu AK (2021) Green Synthesis: An Ecofriendly Route for the Synthesis of Iron Oxide Nanoparticles. Front. Nanotechnol. 3:655062. doi: 10.3389/fnano.2021.655062

[12] Kiwumulo, H. F, Haruna Muwonge1,4, Charles Ibingira2 , Michael Lubwama3 , John Baptist Kirabira3 and Robert Tamale Ssekitoleko (2022). Green synthesis and characterization of iron-oxide nanoparticles using Moringa oleifera: a potential protocol for use in low and middle income countries. BMC Research Notes (2022) 15:149. 15:149 https://doi.org/10.1186/s13104-022-06039-7

[13] Abdulrahman, F; Inyang, I. S; Abbah, J; Binda, L; Amos, S and Gamaniel, K (2004). Effect of Aqueous Leaf Extract of Irvingia Gabonensis on Gastrointestinal Tract in Rodents. Indian Journal of Experimental Biology. 2(8):787-91.

[14] Buarki, F; H. AbuHassan, F. Al Hannan, F. Z. Henari. Green Synthesis of Iron Oxide Nanoparticles Using *Hibiscus rosa sinensis* Flowers and Their Antibacterial Activity. *Journal of Nanotechnology*, vol. 2022, Article ID 5474645, 6 pages, 2022. https://doi.org/10.1155/2022/5474645

[15] Namasivayam, C., and Yamuna, R. T. (1992). Removal of congo red from aqueous solutions by biogas waste slurry. *Journal of Chemical Technology and Biotechnology*, *53*(2), 153-157.

[16] Horsfall, M. Jnr.; and Spiff, A. I. (2005). Sorption of Lead, Cadmium, and Zinc on Sulfur-Containing Chemically Modified Wastes of Fluted Pumpkin (*Telfaria occidentalis)* HOOK f.). *Chem. & Biodiversity; Vol. 2; pp 373 – 385.*

[17] Horsfall, M. Jnr, F. E. Ogban, and E. E. Akporhonor (2005). Biosorption of Pb^{2+} from Aqueous Solution by *Rhizophora mangle* Aerial Root Waste Biomass. *Chemistry & Biodiversity* Vol 2 No 9 1246 – 1255

[18] Adowei, A; Abia, A. A. (2016). Chemical

Oxygen Demand (COD) Attenuation of Methyl Red in Water using Biocarbons obtained from Nipa Palm Leaves. J. Appl. Sci. Environ. Manage. 20 (4) 1163-1176

[19] Ebong, Sifon Emem, Adowei, Pereware, and Obuzor, Gloria Ukalina. (2020). Phytosynthesis and Characterization of Iron Nanocomposites by Irvingia Gabonensis (Ogbono) Aqueous and Ethanol Leaf Extracts. *International Journal of Research* 8(5), 256-265.

[20] Tarawou, T. and Horsfall, M. Jnr (2007). Adsorption of Methylene Blue Dye on Pure and Carbonized Water Weeds. *Bioremediation Journal Vol 11 No 2,1 – 8.* USA

[21] Namasivayam, C., and Arasi, D. J. S. E. (1997). Removal of congo red from wastewater by adsorption onto waste red mud. *Chemosphere*, *34*(2), 401-417.

[22] Preethi, S., Sivasamy, A., Sivanesan, S., Ramamurthi, V., & Swaminathan, G. (2006). Removal of safranin basic dye from aqueous solutions by adsorption onto corncob activated carbon. *Industrial & engineering chemistry research*, *45*(22), 7627-7632.

[23] Adowei, P; Ebong, S. E; Obuzor, G. U (2021). Equilibrium, Kinetic and Thermodynamic Studies of Dyes in Aqueous Solution onto Iron Nanocomposite Stabilized by *Irvingia gabonensis* Leaf Extract. *J. Appl. Sci. Environ. Manage.* Volume. 25 (12) 2071-2083

[24] Purkait, M. K., Maiti, A., DasGupta, S., & De, S. (2007). Removal of congo red using activated carbon and its regeneration. *Journal of Hazardous Materials*, *145*(1), 287-295.

[25] Chen, Y. M., Tsao, T. M., & Wang, M. K. (2011). Removal of crystal violet and methylene blue from aqueous solution using soil nano-clays. In *International conference on environment science and engineering, IPCBEE* (Vol. 8, pp. 252-254).

[26] Adeyemo, A. A., Adeoye, I. O., & Bello, O. S. (2017). Adsorption of dyes using different types of clay: a review. *Applied Water Science*, *7*(2), 543-568.

[27] Ponder, S. M., Darab, J. G., & Mallouk, T. E. (2000). Remediation of Cr (VI) and Pb (II) aqueous solutions using supported, nanoscale zero-valent iron. *Environmental Science & Technology*, *34*(12), 2564-2569.

[28] Lin, C. J., Lo, S. L., & Liou, Y. H. (2005). Degradation of aqueous carbon tetrachloride by nanoscale zerovalent copper on a cation resin. *Chemosphere*, *59*(9), 1299-1307.

[29] Xiong, Z., Zhao, D., and Pan, G. (2007). Rapid and complete destruction of perchlorate in water and ion-exchange brine using stabilized zero-valent iron nanoparticles. *Water research*, *41*(15), 3497-3505.

[30] Wu, S. J., Liou, T. H., and Mi, F. L. (2009). Synthesis of zero-valent copper-chitosan nanocomposites and their application for treatment of hexavalent chromium. *Bioresource technology*, *100*(19), 4348-4353.

[31] Xu, X., Wang, Q., Choi, H. C., and Kim, Y. H. (2010). Encapsulation of iron nanoparticles with PVP nanofibrous membranes to maintain their catalytic activity. *Journal of membrane Science*, *348*(1), 231-237.

[32] Wang, Q., Qian, H., Yang, Y., Zhang, Z., Naman, C., and Xu, X. (2010). Reduction of hexavalent chromium by carboxymethyl cellulose-stabilized zero-valent iron nanoparticles. *Journal of contaminant*

hydrology, *114*(1), 35-42.

[33] Liu, T., Zhao, L., Sun, D., & Tan, X. (2010). Entrapment of nanoscale zero-valent iron in chitosan beads for hexavalent chromium removal from wastewater. *Journal of hazardous materials*, *184*(1), 724-730.

[34] Liu, Z., & Zhang, F. S. (2010). Nano-zerovalent iron contained porous carbons developed from waste biomass for the adsorption and dechlorination of PCBs. *Bioresource technology*, *101*(7), 2562-2564.

[35] Saif, S., Tahir, A., and Chen, Y. (2016). Green synthesis of iron nanoparticles and their environmental applications and implications. *Nanomaterials*, *6*(11), 209.

[36] Sayyad, A. S., Balakrishnan, K., Ci, L., Kabbani, A. T., Vajtai, R., & Ajayan, P. M. (2012). Synthesis of iron nanoparticles from hemoglobin and myoglobin. *Nanotechnology*, *23*(5), 055602.

[37] Siskova, K. M., Straska, J., Krizek, M., Tucek, J., Machala, L., & Zboril, R. (2013). Formation of zero-valent iron nanoparticles mediated by amino acids. *Procedia Environmental Sciences*, *18*, 809-817.

[38] Oben, J. E. (2011). Seed Extract of the West African Bush Mango (Irvingia Gabonensis) and its Use in Health. Nuts and Seeds in Health and Disease Prevention pp. 1187-1189 https://doi.org/10.1016/B978-0-12-375688-6.10140-9

[39] Abdelrahman Mohamed; R. R. Atta; Amna A. Kotp; Fatma I. Abo El-Ela; Hany Abd El-Raheem; Ahmed Farghali; Dalal Hussien M. Alkhalifah; Wael N. Hozzein; Rehab Mahmoud (2023). Green synthesis and characterization of iron oxide nanoparticles for the removal of heavy metals (Cd^{2+} and Ni^{2+}) from aqueous solutions with Antimicrobial Investigation Scientific Reports 13:7227

[40] Okogun, Joseph I. (2002). Drug discovery through ethnobotany in Nigeria: some results. Advances in Phytomedicine. 1. 145-154

[41] Ngondi, J. L., Oben, J. E., & Minka, S. R. (2005). The effect of Irvingia gabonensis seeds on body weight and blood lipids of obese subjects in Cameroon. *Lipids in health and Disease*, *4*(1), 12

[42] Mgbemena, Nkoli Marynnn; Ilechukwu, Ifenna; Okwunodolu, Felicia Uchechukwu; Chukwurah, Joe-Vera, Ogugua and Lucky, Isioma Blessing (2019). Chemical composition, proximate and phytochemical analysis of *Irvingia gabonensis* and *Irvingia wombolu* peels, seed coat, leaves and seeds. Ovidius University Annals of Chemistry. 30 (1): 65 - 69, 2019

[43] Dada, A. O., Adekola, F. A., & Odebunmi, E. O. (2015). A novel zerovalent manganese for removal of copper ions: synthesis, characterization and adsorption studies. *Applied Water Science*, *7*(3), 1409-1427

[44] Karima, B., Mossab, B. L., and A-Hassen, M. E. (2015). Removal of methylene blue from aqueous solutions using an acid activated Algerian bentonite: equilibrium and kinetic studies. In *International renewable energy congress* (pp. 1-8).

[45] Phenrat, T., Saleh, N., Sirk, K., Tilton, R. D., & Lowry, G. V. (2007). Aggregation and sedimentation of aqueous nanoscale zerovalent iron dispersions. *Environmental Science & Technology*, *41*(1), 284-290.

[46] Wang, S., & Zhu, Z. H. (2007). Effects of

acidic treatment of activated carbons on dye adsorption. *Dyes and Pigments*, *75*(2), 306-314.

[47] Kumar, K. M., Mandal, B. K., Kumar, K. S., Reddy, P. S., & Sreedhar, B. (2013). Biobased green method to synthesise palladium and iron nanoparticles using Terminalia chebula aqueous extract. *Spectrochimica Acta Part A: Molecular and Biomolecular Spectroscopy*, *102*, 128-133.

[48] Shahbeig, H., Bagheri, N., Ghorbanian, S. A., Hallajisani, A., & Poorkarimi, S. (2013). A new adsorption isotherm model of aqueous solutions on granular activated carbon. *World Journal of Modeling and. Simulation*, *9*, 243-254.

[49] Youssef, A. M., Dawy, M. B., Akland, M. A., & Abou-Elanwar, A. M. (2013). EDTA versus nitric acid modified activated carbon for adsorption studies of lead (II) from aqueous solutions. *Journal of Applied Sciences Research, 9*, 897-912.

[50] Shaibu, S. E., Adekola, F. A., Adegoke, H. I., and Ayanda, O. S. (2014). A comparative study of the adsorption of methylene blue onto synthesized nanoscale zero-valent iron-bamboo and manganese-bamboo composites. *Materials*, *7*(6), 4493-4507.

[51] Jie Ma; Yuan Zhuang; and Fei Yu (2015). Equilibrium, kinetic and thermodynamic adsorption studies of organic pollutants from aqueous solution onto CNT/C@Fe/chitosan composites. New Journal of Chemistry. 12: 9035 - 9986

[52] Haitham, K; S. Razak, M. A. Nawi (2019). Kinetics and isotherm studies of methyl orange adsorption by a highly recyclable immobilized polyaniline on a glass plate. Arabian Journal of Chemistry. Volume 12, Issue 7, November 2019, Pages 1595-1606

[53] Fouad Krika & Omar el Farouk Benlahbib (2015) Removal of methyl orange from aqueous solution via adsorption on cork as a natural and low-coast adsorbent: equilibrium, kinetic and thermodynamic study of removal process, Desalination and Water Treatment, 53:13, 3711-3723,

[54] Alghamdi, H.M., Abutalib, M.M., Rajeh, A. (2022). Effect of the Fe_2O_3/TiO_2 Nanoparticles on the Structural, Mechanical, Electrical Properties and Antibacterial Activity of the Biodegradable Chitosan/Polyvinyl Alcohol Blend for Food Packaging. *J Polym Environ* 30, 3865–3874https://doi.org/10.1007/s10924-022-02478-2

[55] Jiang, R; Zhu, H. and Yongqian Fu (*2011)*, "Equilibrium and Kinetic studies on adsorption of methyl orange from aqueous solution on chitosan/kaolin/γ-Fe2O3 nanocomposite," *2011 International Conference on Remote Sensing, Environment and Transportation Engineering*, Nanjing, 2011, pp. 7565-7568, doi: 10.1109/RSETE.2011.5966122.

[56] Zhang, D; Ma X-l, Gu Y, Huang, H and Zhang G-w (2020) Green Synthesis of Metallic Nanoparticles and Their Potential Applications to Treat Cancer. *Front. Chem.* 8:799. doi: 10.3389/fchem.2020.00799

[57] Enenebeaku, Conrad K; Nnaemeka J. Okorocha, Uchechi E. Enenebeaku, Ikechukwu C. Ukaga (2017). Adsorption and Equilibrium Studies on the Removal of Methyl Red from Aqueous Solution Using White Potato Peel Powder. *International Letters of Chemistry, Physics and Astronomy*. 72. 52-64

[58] Equbal Ahmad Khan; Shahjahan Tabrez; Alam

Khan (2018). Adsorption of methyl red on activated carbon derived from custard apple (*Annona squamosa*) fruit shell: Equilibrium isotherm and kinetic studies. *Journal of Molecular Liquids*. 249 (1) 1195-1211

[59] Nazia Rahman, Nirmal Chandra Dafader, Abdur Rahim Miah & S. Shahnaz (2019) Efficient removal of methyl orange from aqueous solution using amidoxime adsorbent, International Journal of Environmental Studies, 76:4, 594-60

[60] Atkins, P.W. (1995) Physical Chemistry. 5th Edition, Oxford University Press, Oxford.

[61] Wong K.K., Cheung S.O., Huang L., Niu J., Tao C., Ho C.M., Che C.M., Tam P.K. Further evidence of the anti-inflammatory effects of silver nanoparticles.C*hem. Med. Chem.*2009; 4:1129–1135. doi: 10.1002/cmdc.200900049.

[62] Boparai, Hardiljeet K; Meera Joseph, Denis M. O'Carroll (2011). Kinetics and thermodynamics of cadmium ion removal by adsorption onto nano zerovalent iron particles. *Journal of Hazardous Materials*. 186: 458-46

[63] Ayanda, O. S., Fatoki, O. S., Adekola, F. A., & Ximba, B. J. (2013). Kinetics and equilibrium models for the sorption of tributyltin to nZnO, activated carbon and nZnO/activated carbon composite in artificial seawater. *Marine pollution bulletin*, *72*(1), 222-230.

[64] Hao, Y. M., Man, C., & Hu, Z. B. (2010). Effective removal of Cu (II) ions from aqueous solution by amino-functionalized magnetic nanoparticles. *Journal of Hazardous Materials*, *184*(1), 392-399.

[65] Lisha KP, Maliyekkal SM and Pradeep T (2010) Manganese dioxide nanowhiskers: A potential adsorbent for the removal of Hg(II) from water. Chemical Engineering Journal 160: 432–439.